Supplementary Information

Lin-Lin Zhang,[a] Cheng-Bing Zhong,[a] Ting-Jing Huang,[a] Li-Min Zhang,[b] Feng Yan[b] and Yi-Lun Ying[*acd]

[a] Molecular Sensing and Imaging Center, School of Chemistry and Chemical Engineering, Nanjing University, Nanjing 210023 (P.R. China).

[b] School of Electronic Science and Engineering, Nanjing University, Nanjing 210023 (P.R. China).

[c] State Key Laboratory of Analytical Chemistry for Life Science, Nanjing University, Nanjing 210023 (P.R. China).

[d] Chemistry and Biomedicine Innovation Center, Nanjing University, Nanjing 210023 (P.R. China).

Corresponding author

E-mail: yilunying@nju.edu.cn

Keywords: nanopore; single molecule detection; microchip; droplet sensing; biomarker

Table of Contents

Supplementary Tables

Table S1 Single-molecule techniques for single biomarker detection.

| Methods	Sample volume	Limit of detection	Channel	Ref.
Single‑molecule Fluorescence	25 µL	100 fM	N.A.	1
Droplet Digital ELISA	2 µL (pL droplet)	20 aM	N.A.	2
AFM	30 µL	0.1 µM	1	3
Electronic FET	50 µL	10 µM	1	4
Conventional Nanopore	1 mL	0.1 µM	1	5
Oxford Nanopore Sequencing	250 µL	2-4 µg	512	6
Ag/AgCl-supported Nanopore	10 µL	0.1 µM	1	7
Droplet Nanopore	1 µL	N.A.	1	8
Droplet Nanopore	0.4 µL	~50 pg (0.1 µM)	16	This work

Supplementary Figures
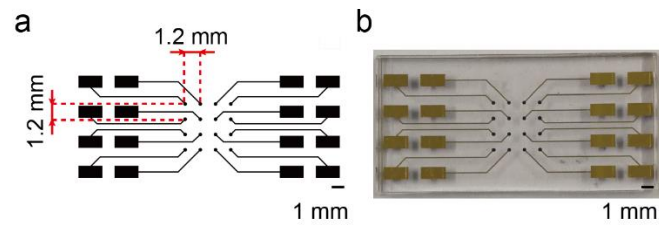
Fig. S1 The design of 16-channel microchip. (a) The sketch image. (b) The optical image. The design of pattern aims to connect to the Orbit 16 instrument (Nanion Technologies GmbH, Munich, Germany) for 16-channel recording. Comparable to MECA-16 (Ionera Technologies GmbH, Freiburg, Germany, available through Nanion Technologies GmbH), the spacing of microwells was increased to 1.2 mm. This design facilitates the efficient operation of membrane formation on each channel.
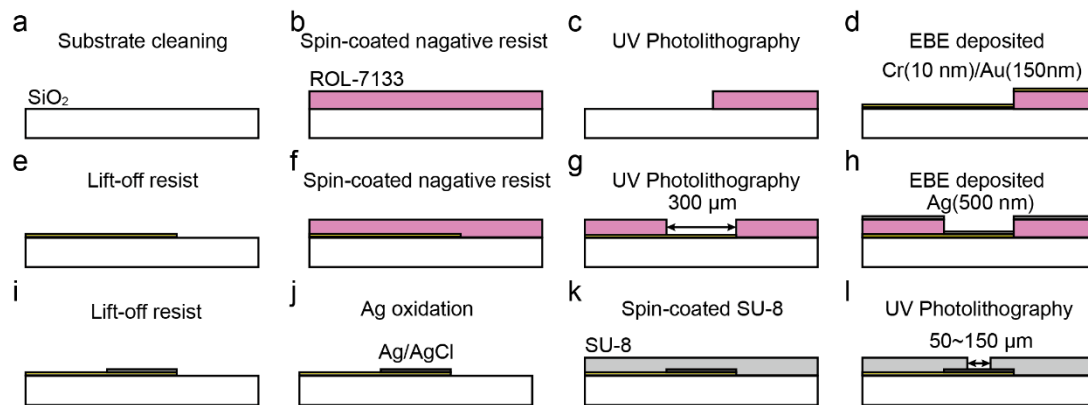
Fig. S2 The fabrication steps for the designed microchip. (a) Substrate cleaning. (b) Spin-coated negative resist. (c) UV photolithography. (d) Cr/Au Deposition. (e) Lift-off resist. (f) Spin-coated negative resist. (g) UV photolithography. (h) Ag Deposition. (i) Lift-off resist. (j) Ag oxidation. (k) Spin-coated SU-8 resist. (l) UV photolithography. Schematically shown with one microwell on the cross-sectional view.
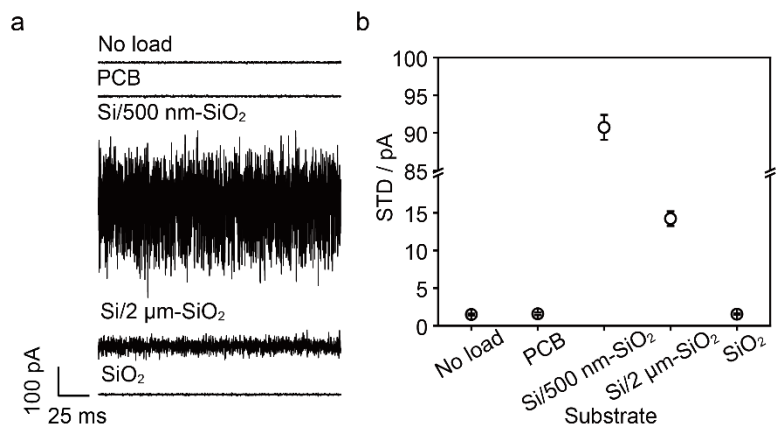
4

Fig. S3 The open circuit current from various substrates. (a) The raw current traces. From top to bottom: no load, printed circuit board (PCB), Si/500 nm-SiO_2, Si/2 μm-SiO_2, and SiO_2. (b) The Standard deviation (STD) of open circuit current for various substrates. Error bars depict the STD of 3 independent measurements. The SiO_2 behaves the lowest noise performance among these substrates. The data was acquired with 2 nA ranging, 5 kHz filtering and 100 kHz sampling rate using an Orbit 16 instrument.
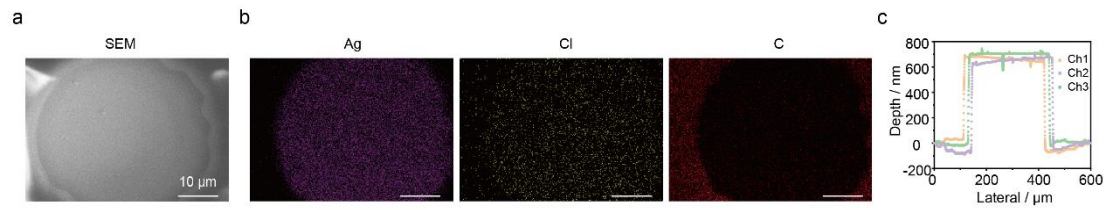
Fig. S4 The characterization of the fabricated Ag/AgCl microelectrode on the microchip. (a) The SEM image of the Ag/AgCl microelectrode with the diameter of 50 μm. The non-conducting edge is the SU-8 layer. The morphology of SU-8 layer is affected under the electron beam irradiation. (b) The corresponding SEDX elemental mapping of the Ag/AgCl microelectrode. The Ag and Cl elements were evenly distributed in the Ag/AgCl electrode while the C element indicates the coated SU-8 layer. Scale bar is 10 μm. (c) The profile of three Ag/AgCl microelectrodes from one microchip. The height of the Ag/AgCl microelectrode on the SiO_2 substrate is 682 ± 5 nm.
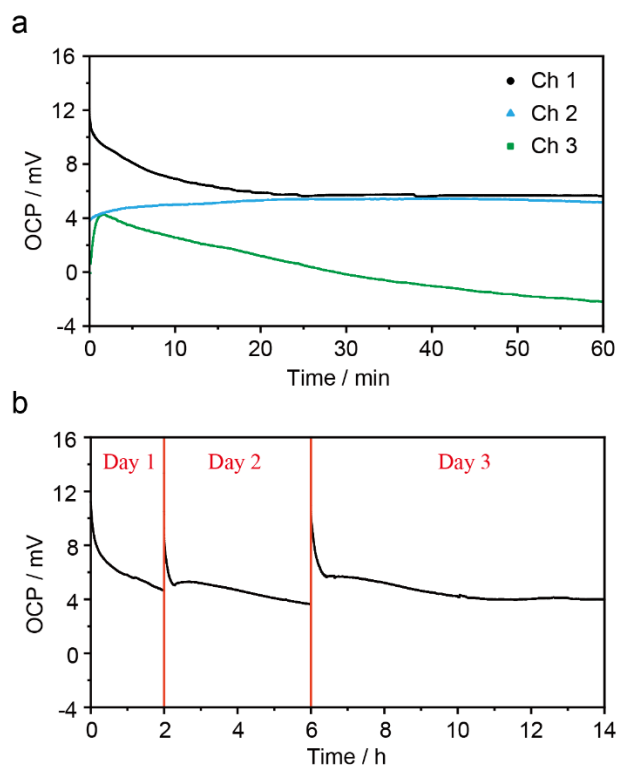
Fig. S5 The open-circuit potential (OCP) of Ag/AgCl microelectrodes *vs.* a commercial Ag/AgCl reference electrode. (a) The OCP of 3 independent Ag/AgCl microelectrodes from one nanopore microchip. Black: Channel 1 (Ch1); Blue: Channel 2 (Ch2); Green: Channel 3 (Ch3). (b) The OCP of Ch 1 from 3 consecutive days. Each measurement requires a minimum of 2 hours of daily recording. All OCP was a slightly higher than the theoretical value of zero and the begin value shown fluctuation during the first 10 s, which may be attributed to imperfect chlorination, the concentration differences of Cl⁻, and the uncertain junction potentials, as described in a previous report[9]. The data was acquired *vs.* a commercial Ag/AgCl reference electrode, obtained from Wuhan Brain Link Technology (Wuhan, China), in 1.0 M KCl, 10.0 mM Tris with 1.0 mM EDTA at pH 8.0 using the CHI instrument.
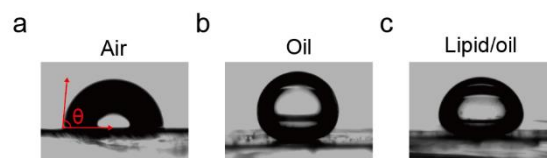
Fig. S6 The contact angle measurement of the 3 μL ultrapure water droplet on the SU-8 surface. The measured contact angle θ is (a) 88.3 ± 3.4° in air, (b) 150.3 ± 1.5° in the oil mixture containing of 1:1 (v/v) hexadecane and silicone AR 20, and (c) 147.2 ± 2.4° in the solution containing of 10 mg/mL DPhPC in 1:1 hexadecane and silicone AR 20 (v:v).
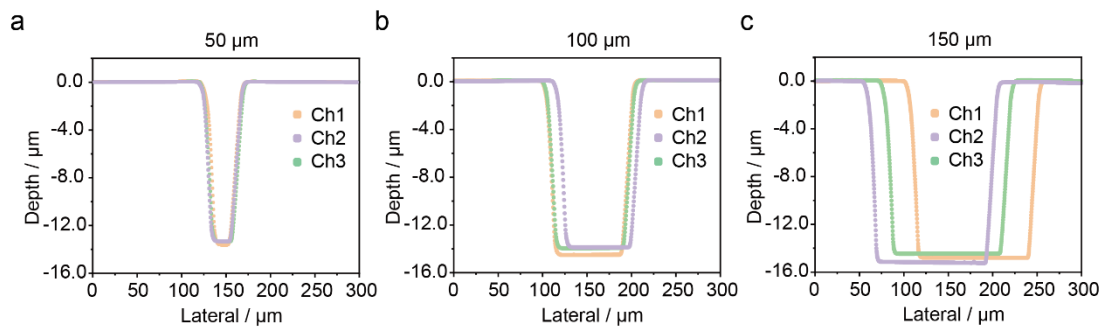
Fig. S7 The profile of microwells measured by the step profiler. The microwells with diameters of (a) 50 μm, (b) 100 μm, and (c) 150 μm on the 3 independent microchips. Each microchip was measured with 3 independent channels (Ch1, Ch2 and Ch3, respectively). The depths and surface profiles of the microwells are consistent, even under various diameters.
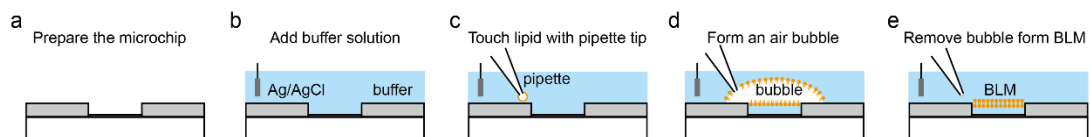
Fig. S8 Air bubble method for the formation of Black Lipid Membrane (BLM). (a) Prepare the microchip, (b) fill the buffer solution, (c) pipette an air bubble which was dipped with lipid solution, (d) spread the air bubble on the microwell, (e) remove the air bubble and leave the lipid membrane at the top surface of the microwell. Schematically shown with one microwell on the cross-sectional view.
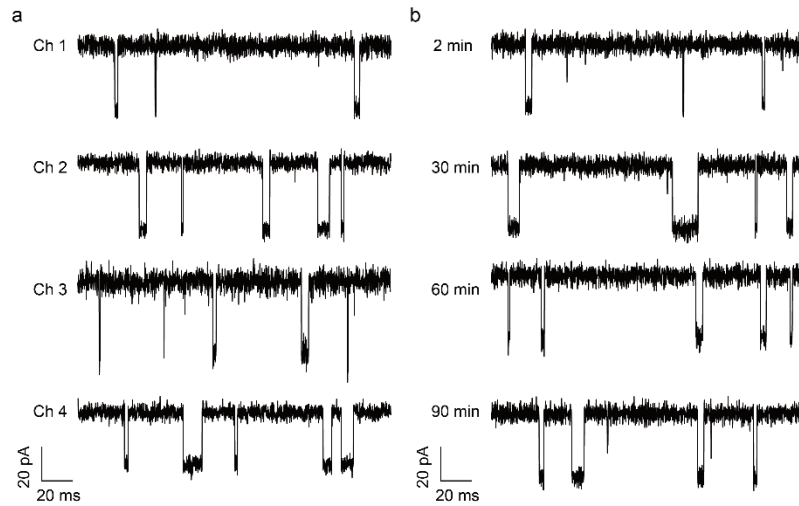
Fig. S9 The raw current trace of Poly(dA)$_4$ (5'-AAAA-3', dA$_4$) detection with the wild-type (WT) Aerolysin (AeL) by using air bubble method. (a) Multichannel recording of 4 independent channels on a single microchip. (b) The raw current trace with long recording time. From up to bottom: the represented current trace at the recording time of 2 min, 30 min, 60 min and 90 min. All data were acquired on the homemade microchip with the diameter of microwells at 50 μm, at the applied voltage of + 100 mV in 1.0 M KCl, 10.0 mM Tris, and 1.0 mM EDTA at pH 8.0 with 5 kHz filtering and 100 kHz sampling rate using the Orbit 16 instrument.
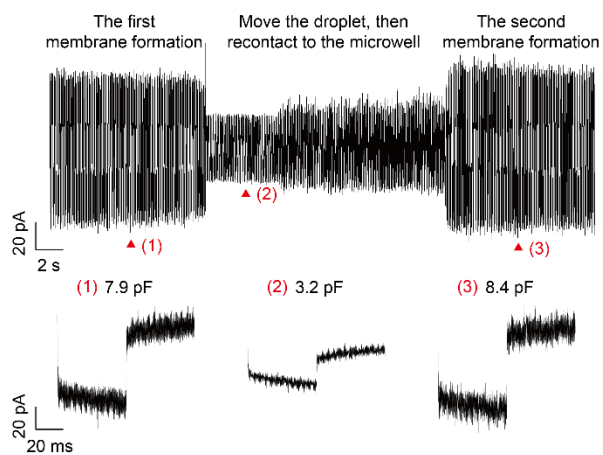
Fig. S10 The capacitance changes during the membrane reformation by moving the 1 μL droplet around on the 50 μm microwells. After the first membrane formation step (top, left), it can be reformed by relocating the droplet (top, middle) and recontacting the droplet to the microwells to form the membrane again (top, right). In the middle step, due to the droplet movement, there was an increase in noise. The red triangles denote typical current traces and capacitances during the capacitance measurement (bottom). All data were acquired at the applied triangular voltage with an amplitude of ± 100 mV and a frequency of 10 Hz in 1.0 M KCl, 10.0 mM Tris, and 1.0 mM EDTA at pH 8.0 with 5 kHz filtering and 100 kHz sampling rate using an Orbit 16 instrument.
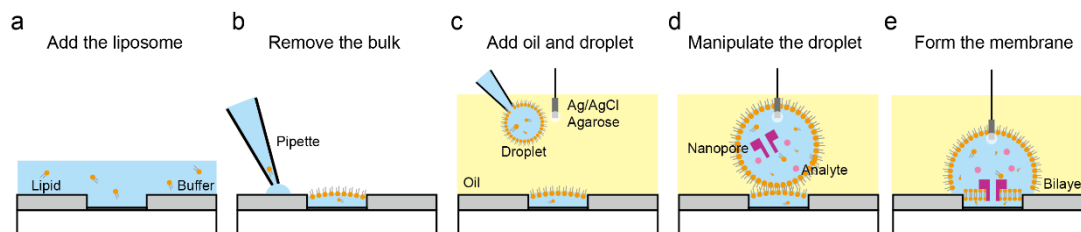
Fig. S11 Formation procedure using "lipid-in" droplet method. (a) Fill the liposome solution which contains of the lipid and buffer solution; (b) remove the redundant solution and only left the solution in the microwell; (c) add the oil and pipette the droplet into the end of agarose-coated Ag/AgCl electrode; and (d) move the droplet onto the microwell for (e) bilayer lipid membrane formation and nanopore sensing.
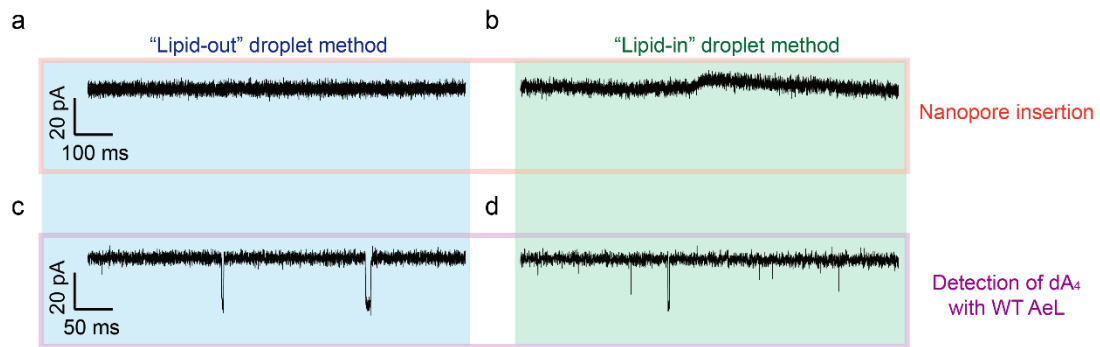
Fig. S12 The typical current trace using "lipid-out" droplet method and "lipid-in" droplet method on the MECA-16 chip within a 2 μL droplet. The open-pore current with single WT AeL insertion using (a) "lipid-out" and (b) "lipid-in" method, respectively. The current trace using "lipid-in" droplet method shown fluctuation. The typical current trace of 1 μM dA_4 detection with WT AeL using (c) "lipid-out" and (d) "lipid-in" method, respectively. All data were acquired at + 100 mV in 1.0 M KCl, 10.0 mM Tris, and 1.0 mM EDTA at pH 8.0 with 5 kHz filtering and 100 kHz sampling rate using an Orbit 16 instrument.
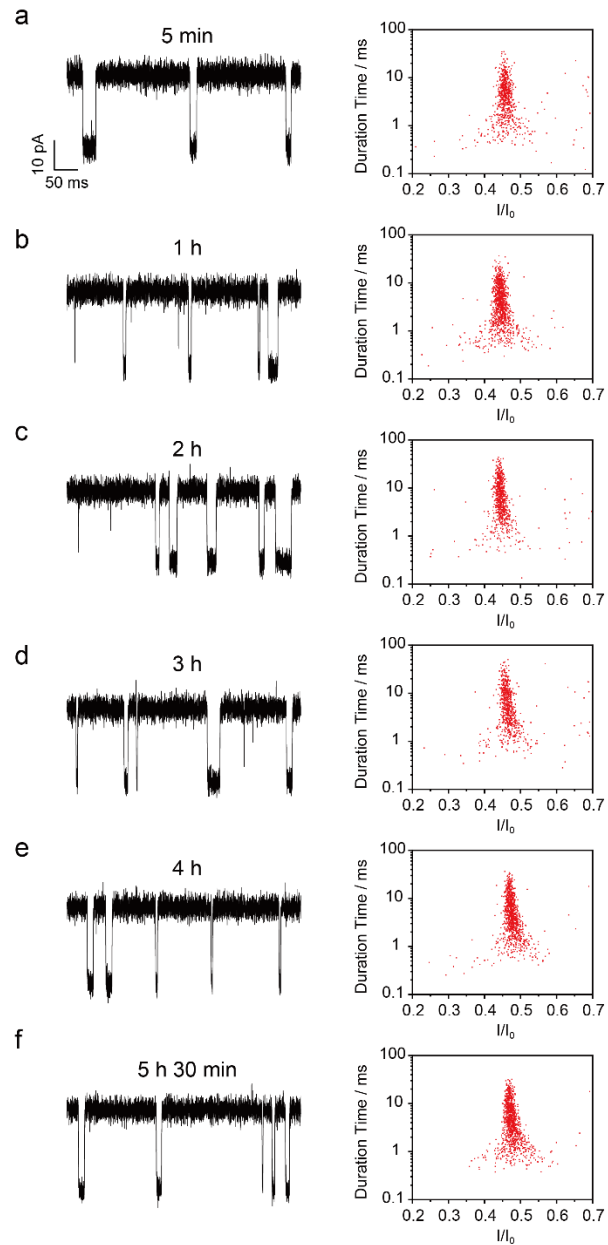
Fig. S13 The more than 5 h current recording for 1 μM Poly(dA)$_4$ detection with WT AeL within a 2 μL droplet. The typical current traces (Left) and scatter plots (Right) for Poly(dA)$_4$ detection at 5 min (a), 1 h (b), 2 h (c), 3 h (d), 4 h (e), and 5 h 30 min (f), respectively. The results were acquired and counted at + 100 mV for 5 min, in the electrolyte solution of 1.0 M KCl, 10.0 mM Tris, and 1.0 mM EDTA at pH 8.0 with 5 kHz filtering and 100 kHz sampling rate using the MECA-16 chip and Orbit 16 instrument.
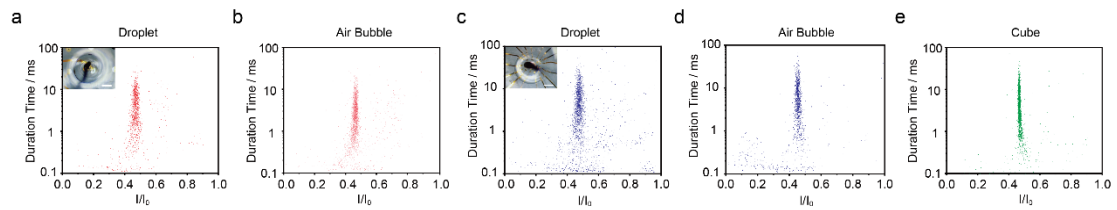
Fig. S14 The scatter plots of 1 μM Poly(dA)$_4$ detection with WT AeL. The "Lipid-out" droplet method (a) and air bubble method (b) for membrane formation on the homemade microchip featuring microwells with a diameter of 50 μm using the Orbit 16 instrument. The "Lipid-out" droplet method (c) and air bubble method (d) for membrane formation on the commercial MECA-16 chip with microwells featuring a diameter of 50 μm using the Orbit 16 instrument. The insert in (a), (c) is the 2 μL droplet on the microchip for nanopore sensing and the scale bar is 500 μm. (e) The 1 μM dA$_4$ detected with WT AeL using lab-designed instrument Cube[10]. The results were acquired at + 100 mV for 5 min, in the electrolyte solution of 1.0 M KCl, 10.0 mM Tris, and 1.0 mM EDTA at pH 8.0 with 5 kHz filtering and 100 kHz sampling rate.
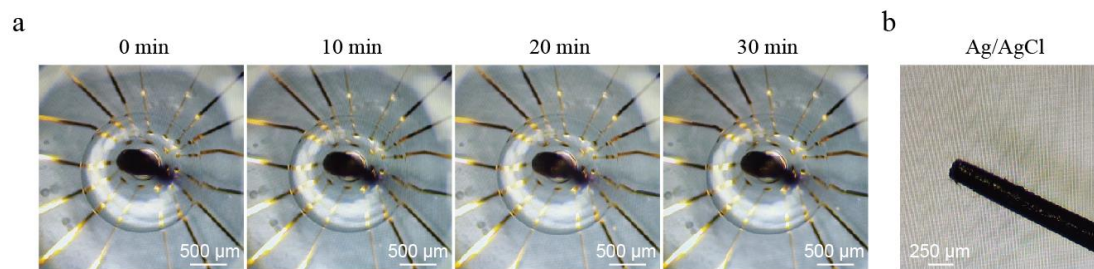
Fig. S15 The 2 μL droplet containing of 3.0 M KCl, 10.0 mM Tris, and 1.0 mM EDTA at pH 8.0 inserted with Ag/AgCl electrode. (a) Optical images of 2 μL droplet system for 30 min sensing. The scale bar is 500 μm. (b) Optical images of a 0.25 mm diameter Ag/AgCl electrode coated with agarose after recording for 30 minutes. The scale bar is 250 μm.
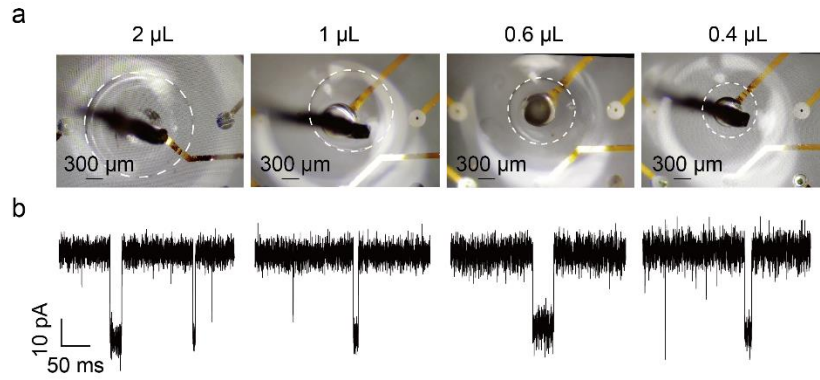
Fig. S16 The "lipid-out" droplet method for nanopore sensing on the homemade microchip with microwells of 50 μm diameter. (a) The optical pictures and (b) typical current traces of various droplets volumes ranging from 2 μL to 0.4 μL. The white circles indicate the droplets. As the droplet volume decreased, the quality of dA_4 declined from 254 pg to 51 pg. All data were acquired with 0.1 μM dA_4 detection by WT AeL at + 100 mV, in the electrolyte solution of 1.0 M KCl, 10.0 mM Tris, and 1.0 mM EDTA at pH 8.0 with 5 kHz filtering and 100 kHz sampling rate using an Orbit 16 instrument.
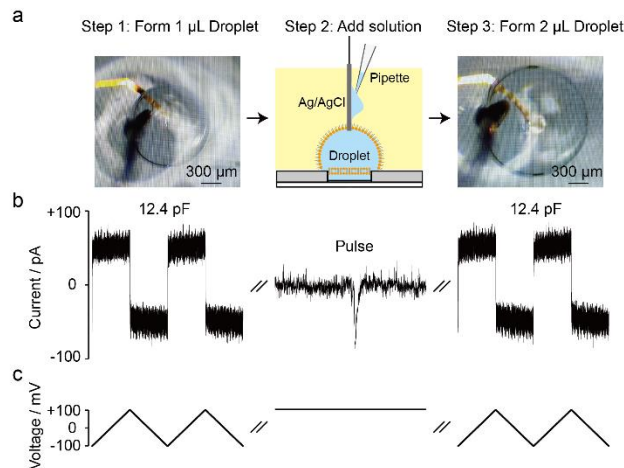
Fig. S17 The sample addition process using the droplet nanopore microchip. (a) The optical images and schematic for adding 1 μL of buffer solution into a droplet with a volume of 1 μL. (b) The current trace during the membrane capacitance measurement and droplet addition. With the 1 μL droplet for membrane formation, the capacitance of the membrane was 12.4 pF (Left). Pulse signal and noise display for another 1 μL solution added into the droplet at + 100 mV (Middle). After a few minutes for membrane stabilization, the capacitance was 12.4 pF, indicating the bilayer membrane had formed again (Right). (c) The applied voltage. Apply a triangular voltage with an amplitude of ± 100 mV and a frequency of 10 Hz for capacitance measurement. All data were acquired in 1.0 M KCl, 10.0 mM Tris, and 1.0 mM EDTA at pH 8.0 with 5 kHz filtering and 100 kHz sampling rate using the homemade microchip featuring microwells with diameters of 50 μm and Orbit 16 instrument.
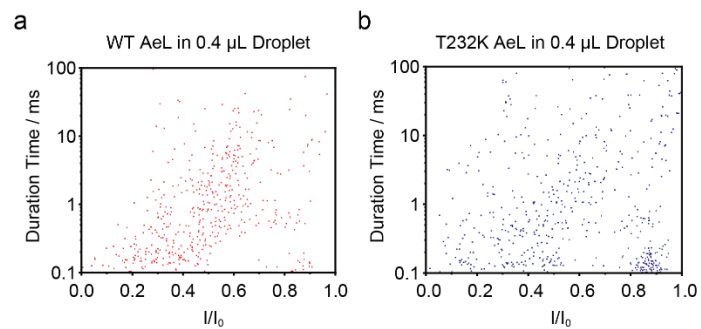
Fig. S18 The scatter plots of nanopore current recording using "lipid-out" droplet method. The scatter plots of background signals by (a) WT AeL nanopore (607 events) and (b) T232K AeL (603 events) using 0.4 μL droplet for 10 min on the homemade microchips with the microwells of 50 μm diameter. The data was acquired at + 100 mV, in the electrolyte solution of 1.0 M KCl, 10.0 mM Tris, and 1.0 mM EDTA at pH 8.0 with 5 kHz filtering and 100 kHz sampling rate using an Orbit 16 instrument.

References

1. H. Zhang, Y. Liu, K. Zhang, J. Ji, J. Liu and B. Liu, *Anal. Chem.*, 2018, **90**, 9315–9321.
2. L. Cohen, N. Cui, Y. Cai, P. M. Garden, X. Li, D. A. Weitz and D. R. Walt, *ACS Nano*, 2020, **14**, 9491-9501.
3. Y. D. Ivanov, T. O. Pleshakova, I. D. Shumov, A. F. Kozlov, I. A. Ivanova, A. A. Valueva, V. Y. Tatur, M. V. Smelov, N. D. Ivanova and V. S. Ziborov, *Sci. Rep.*, 2020, **10**, 9022.
4. W. Liu, J. Li, Y. Xu, D. Yin, X. Zhu, H. Fu, X. Su and X. Guo, *Adv. Sci.*, 2021, **8**, 2101383.
5. J. Jiang, M. Li, X. Wu, Y. Ying, H. Han and Y. Long, *Nat. Chem.*, 2023, **15**, 578-586.
6. S. Scalabrin, G. Magris, M. Liva, N. Vitulo, M. Vidotto, D. Scaglione, L. Del Terra, M. R. Ruosi, L. Navarini, G. Pellegrino, Y. T. J. C. Berny Mier, L. Toniutti, F. Suggi Liverani, M. Cerutti, G. Di Gaspero and M. Morgante, *Nat. Commun.*, 2024, **15**, 463.
7. K. Shoji, R. Kawano and R. J. White, *Anal. Chem.*, 2020, **92**, 10856-10862.
8. R. Strutt, J. W. Hindley, J. Gregg, P. J. Booth, J. D. Harling, R. V. Law, M. S. Friddin and O. Ces, *Chem. Sci.*, 2021, **12**, 2138-2145.
9. B. J. Polk, A. Stelzenmuller, G. Mijares, W. MacCrehan and M. Gaitan, *Sens. Actuators B Chem.*, 2006, **114**, 239-247.
10. Z. Hu, Y. Ying, M. Huo, X. Kong, X. Yu, J. Zhang and Y. Long, *J. Chem. Educ.*, 2020, **97**, 4345-4354.